

SCIENTIFIC REPORTS

OPEN

Direct observation of high spin polarization in Co₂FeAl thin films

Xiaoqian Zhang¹, Huanfeng Xu¹, Bolin Lai¹, Qiangsheng Lu^{2,3}, Xianyang Lu⁴, Yequan Chen¹, Wei Niu¹, Chenyi Gu⁵, Wenqing Liu^{1,4}, Xuefeng Wang¹, Chang Liu², Yuefeng Nie⁵, Liang He¹ & Yongbing Xu^{1,4}

Received: 11 December 2017

Accepted: 3 April 2018

Published online: 23 May 2018

We have studied the Co₂FeAl thin films with different thicknesses epitaxially grown on GaAs (001) by molecular beam epitaxy. The magnetic properties and spin polarization of the films were investigated by *in-situ* magneto-optic Kerr effect (MOKE) measurement and spin-resolved angle-resolved photoemission spectroscopy (spin-ARPES) at 300 K, respectively. High spin polarization of 58% ($\pm 7\%$) was observed for the film with thickness of 21 unit cells (uc), for the first time. However, when the thickness decreases to 2.5 uc, the spin polarization falls to 29% ($\pm 2\%$) only. This change is also accompanied by a magnetic transition at 4 uc characterized by the MOKE intensity. Above it, the film's magnetization reaches the bulk value of 1000 emu/cm³. Our findings set a lower limit on the thickness of Co₂FeAl films, which possesses both high spin polarization and large magnetization.

Spintronic devices rely on thin layers of magnetic materials, for they are designed to control both the charge and the spin current of the electrons. Half-metallic ferromagnets (HMFs) have only one spin channel for conduction at the Fermi level, while they have a band gap in the other spin channel^{1–4}. Therefore, in principle this kind of material has 100% spin polarization for transport, which is perfect for spin injection, spin filtering, and spin transfer torque devices⁵. Among different types of HMFs, Co-based full Heusler alloys have attracted most interests due to their relatively high Curie temperature and low Gilbert damping coefficient^{6–9}.

Although the future of applications is brilliant, most studies of Co₂FeAl films are focused on relatively thicker films of more than 10 nm^{5,10,11}. However, the ultra-thin film is essential for the miniaturization of electronic devices in some aspects. Magnetic tunnel junctions (MTJs) based on Co₂FeAl_{0.5}Si_{0.5}¹² and La_{0.7}Sr_{0.3}MnO₃¹³ have been reported to achieve tunnel magnetoresistance (TMR) ratio of 386% at 300 K and transport spin polarization of 99.6% at 10 K, respectively. However, the device independent investigations on the spin polarization of half metals are limited, and mostly focused on Co₂MnSi^{6,14}. Therefore, in this manuscript, we have explored the magnetic properties and the spin-polarization of the ultra-thin Co₂FeAl films ranging from 1 unit cell (uc) to 35 uc by *in-situ* magneto-optic Kerr effect (MOKE) and spin-resolved angle-resolved photoemission spectroscopy (spin-ARPES)¹⁵ at 300 K.

We have found that the films possess a combination of uniaxial and cubic anisotropy. The magnetization of all the films demonstrates a linear relationship with the thickness and a kink at 4 uc, above which it reaches the bulk value of 1000 emu/cm³ (Fig. S2)¹⁶. This suggests that a bulk magnetization is achieved for Co₂FeAl thin films with a thickness of at least 4 uc. At greater thicknesses, we find a weak thickness dependence of the surface spin polarization at room temperature, which reaches 58% ($\pm 7\%$) for a 21-uc-thick film.

Results

High-quality Co₂FeAl ultra-thin films. The Co₂FeAl films were grown on GaAs (001) by molecular beam epitaxy (MBE). Real-time reflection high energy electron diffraction (RHEED) was used to monitor the *in-situ* growth dynamics with the electron beam along the [110] and [100] directions. Figure 1a,b present the RHEED

¹Jiangsu Provincial Key Laboratory of Advanced Photonic and Electronic Materials, Collaborative Innovation Center of Advanced Microstructures, School of Electronic Science and Engineering, Nanjing University, Nanjing, 210093, China. ²Department of Physics, Southern University of Science and Technology, Shenzhen, Guangdong, 518055, China. ³Department of Physics and Astronomy, University of Missouri, Columbia, MO, 65211, USA. ⁴York-Nanjing Joint Centre (YNJC) for spintronics and nano engineering, Department of Electronics, The University of York, York, YO10 3DD, United Kingdom. ⁵National Laboratory of Solid State Microstructures, College of Engineering and Applied Sciences, and Collaborative Innovation Center of Advanced Microstructures, Nanjing University, Nanjing, 210093, China. Correspondence and requests for materials should be addressed to L.H. (email: heliang@nju.edu.cn) or Y.X. (email: ybxu@nju.edu.cn)

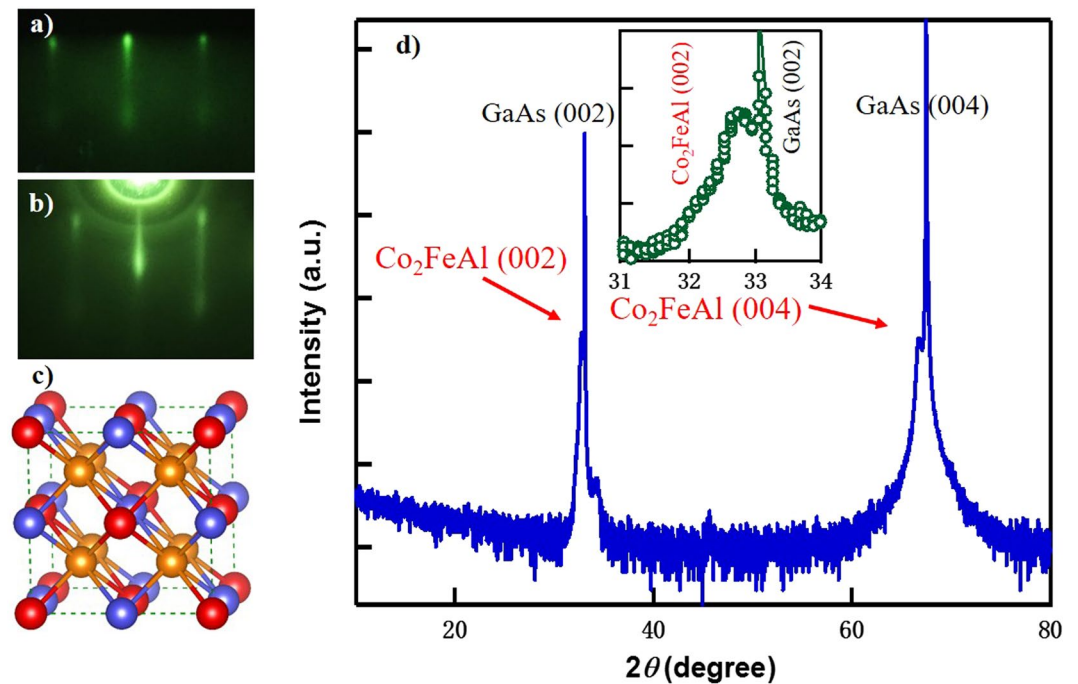


Figure 1. RHEED, structure model and XRD measurements of the Co_2FeAl films. (a) and (b) RHEED patterns of a Co_2FeAl (001) film with the electron beam along [110] & [100], respectively. (c) Schematic representation of Co_2FeAl with L_{21} structure. The golden, purple and red balls denote Co, Al and Fe atoms, respectively. (d) X-ray 2θ - ω diffraction patterns of a 13-uc-thick Co_2FeAl film grown on GaAs (001) substrate. Top inset is a close view of the Co_2FeAl (002) peak.

patterns of an as-grown Co_2FeAl film with a thickness of 20 uc. The sharp streaky lines indicate a flat surface morphology, thus the growth is smoothly pseudomorphic. The epitaxial relationship is Co_2FeAl (001)[110] // GaAs (001)[110]. Figure 1d exhibits X-ray 2θ - ω diffraction pattern of a Co_2FeAl film with a thickness of 13 uc. Though the film is ultra-thin, Co_2FeAl (200) and (400) peaks can still be clearly observed, in addition to the peaks of GaAs substrate. From the diffraction peaks, the lattice constant of the film can be estimated as 5.70 Å, slightly smaller than the theoretical value of 5.727 Å. This suggests that our film is still under compressive strain induced by the GaAs substrate.

In theory, a perfect chemically and structurally ordered Co_2FeAl crystal is L_{21} phase. As exhibited in Fig. 1c, Co atoms (golden balls) sit at the eight vertexes of the cubic, while Fe (red balls) and Al atoms (purple balls) occupy the body center place alternately. It would be characterized by the peaks of superlattice reflections like (111) and (311)^{17,18}. As the Fe and Al atoms mix with each other, B2 phase appears. In our case, the presence of both (200) and (400) peak indicates that our Co_2FeAl films are in the B2 phase¹⁹. Besides the two main peaks, the absence of extra peaks suggests that our films possess a single crystal structure.

***In-situ* longitudinal MOKE measurements.** The magnetic properties of the Co_2FeAl films were probed *in-situ* by MOKE measurements at room temperature. We have measured the longitudinal MOKE along $[\bar{1} 0 0]$, $[\bar{1} 1 0]$, $[0 1 0]$ & $[1 1 0]$ crystal orientations. It is interesting to notice that the magnetization of our Co_2FeAl films exhibit a combination of uniaxial and cubic anisotropy. As the film thickness decreases, the uniaxial anisotropy becomes more pronounced with the easy axis along $[\bar{1} 1 0]$ direction and hard axis at $[1 1 0]$ (Fig. S1). This uniaxial anisotropy may be induced by the $\text{Co}_2\text{FeAl}/\text{GaAs}$ interface, as the dangling bonds at the GaAs surface are all along $[\bar{1} 1 0]$. Along the easy axis, the field dependent MOKE signals (θ_K) of various thicknesses are presented in Fig. 2a. Square hysteresis loops can be observed with thickness down to 1 uc. This strong remanence for 1 uc suggests that the long range ordering has formed between the Co and Fe nanoclusters through the ferromagnetic double exchange couplings²⁰ at the early growth stage. As the film thickness increases, both θ_K and the coercivity increases. The coercivity saturates after the film thickness is beyond 4 uc.

The thickness dependent saturated Kerr rotation and coercive field extracted from Fig. 2a are presented in Fig. 2b,c, respectively. When the thickness increases from 0 to 4 uc, the saturated Kerr rotation increases linearly. And more interestingly, it passes through zero (blue solid line in Fig. 2b), suggesting that there are no magnetic dead layers, and the entire Co_2FeAl film is ferromagnetic at room temperature. At the same time, the coercivity also increases linearly with the thicknesses, as indicated by the blue solid line in Fig. 2c. For thicker films ($t > 4$ uc), the Kerr rotation is also linearly dependent on the film thicknesses, with a smaller slope as fitted by the orange solid line in Fig. 2b. This is because the film thickness is still thinner than the detection depth of MOKE measurement, which is usually 10–50 nm^{16,21}. Thus, the thicker the film is, the stronger the MOKE signal is. On

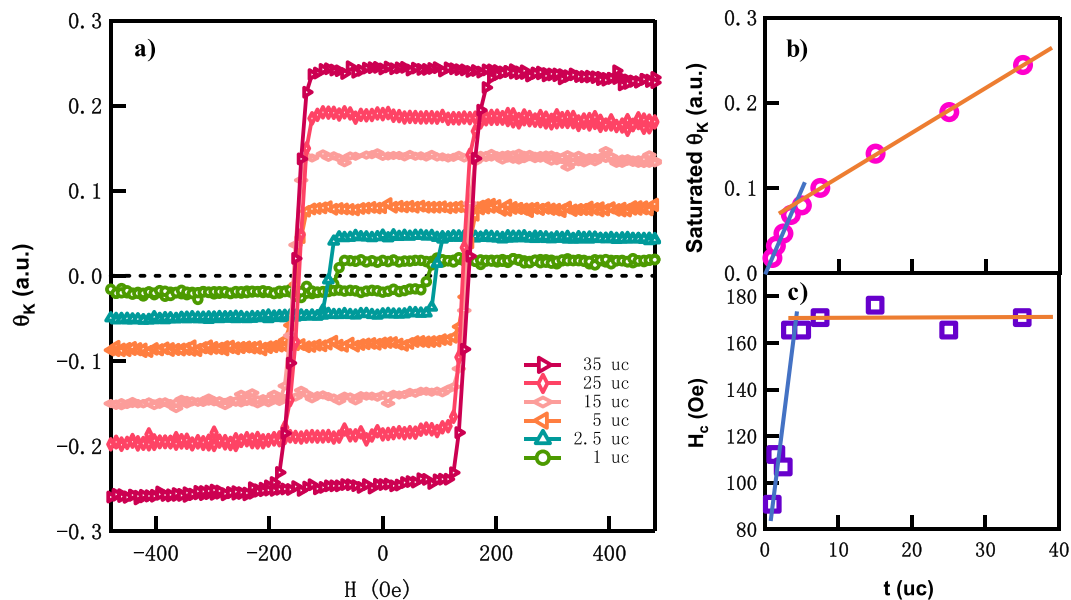


Figure 2. Thickness-dependent *in-situ* MOKE measurements of the Co₂FeAl films. (a) In-plane magnetization measured at 300 K along $[\bar{1} 1 0]$ (easy axis direction) by a longitudinal-mode MOKE set up. Both thickness dependent (b) Kerr rotation and (c) coercive field estimated from (a) show a turning point at ~ 4 uc.

the other hand, the coercivities stay constant (Fig. 2c), which are equal to the bulk value^{22,23}. The magnetization and coercivity imply that the films thicker than 4 uc are bulk-like, while films thinner than 4 uc are mostly affected by the interface¹⁶.

High spin polarization at the Fermi level. To investigate the spin polarization of the Co₂FeAl films, samples were transferred under ultra-high vacuum to the ARPES chamber upon completing the film growth. This *in-situ* ARPES set-up prevents the contamination from ambient environment, thus it gives us a chance to observe the real spin polarization at the fresh Co₂FeAl surface. Prior to the measurements, the magnetization direction was pulled to the easy axis along $[\bar{1} 1 0]$ direction, with an external magnetic field of 500 Oe. During the measurements, no out-of-plane spin polarization was observed, which confirms that the magnetization of our Co₂FeAl films is in plane, as confirmed by our MOKE measurements.

Figure 3 exhibits the representative spin-resolved photoemission spectra and the corresponding spin polarization at room temperature. A broad peak at ~ 1.0 eV in Fig. 3a comes from the combination of Co and Fe's 3d electronic states, which is similar to the spectra of Co₂MnSi films obtained in previous report²¹. The polarization of a free-electron beam can be determined by a spin-sensitive technique that involves scattering measurements from metals with strong spin orbit coupling¹⁴. Thus the spin polarization can be defined as:

$$p = \frac{I^+ - I^-}{I^+ + I^-} S_{eff} \quad (1)$$

I^+ and I^- represent the intensity spectra for majority and minority spins, respectively. S_{eff} means the Sherman function, representing the analyzing power or spin sensitivity of the polarimeter, which is equal to 0.16 ± 0.01 in our case^{14,24}.

The magnitude of spin polarization of ferromagnetic materials is a key property for their application in spintronic devices, especially at room temperature. As shown in Fig. 3b–e, the spin polarization of Co₂FeAl films exhibits a peak at the Fermi energy (E_F), then decreases slowly with the binding energy increasing, and reaches zero beyond 1 eV. For the film of 2.5 uc, the peak value is much lower than the thicker films, and also the spin polarization goes to a negative value at higher binding energies, suggesting the swap of spin direction of the majority and the minority band. From the theoretical calculation²⁵, the Fermi level crosses the majority band, touches the top of minority valence band, indicating the highest spin polarization at the Fermi level, which is in good agreement with our experimental observation. The thickness dependent spin polarization at the Fermi surface is exhibited in Fig. 3f. We find that the spin polarization decreases slowly as the film thickness is reduced from 21 uc to 6 uc, and drops to 29% ($\pm 2\%$) when the film thickness is reduced to 2.5 uc.

Discussion

The spin polarization of 58% ($\pm 7\%$) for the Co₂FeAl films with thickness of 21 uc is the highest value detected directly up to now for this materials system. However, it is still smaller than the expected 100% for half-metallic ferromagnets²¹. The plausible reasons may be local atomic disorder of Fe and Al atoms as demonstrated by XRD measurements or nonstoichiometric phase at the surface^{26,27}. We have to point out that the measured spin

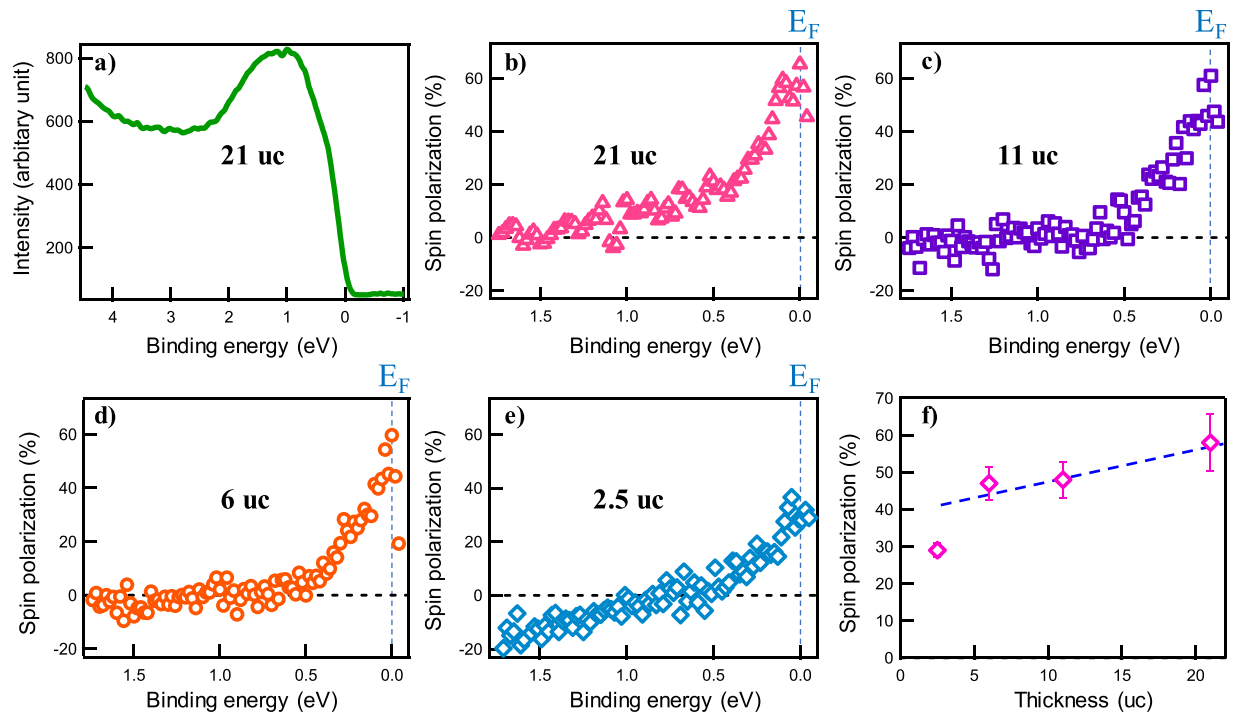


Figure 3. *In situ* spin-resolved ARPES measurements. (a) Spin-resolved photoemission spectra of the 21-uc-thick Co₂FeAl film, probed by 21.2 eV photons at 300 K. (b–e) Spin polarizations of Co₂FeAl films with thicknesses of 21 uc, 11 uc, 6 uc and 2.5 uc, respectively. (f) Spin polarizations at the Fermi level versus film thicknesses. It decreases slowly with film thicknesses decreasing from 21 uc to 6 uc, and then suddenly drops to 29% at 2.5 uc.

polarization is at the interface between the Co₂FeAl bulk and the vacuum, which may not be equal to the spin polarization at the interface between the Co₂FeAl and MgO in a real TMR device. That interface could alter the spin polarization dramatically, as we can see in Fig. 3f. With film thickness decreasing to 2.5 uc, the strong attenuation of the spin polarization happens at E_F, which may be due to the interface bonding or the site disorder, resulting in a spin polarization that is much less than the bulk.

In conclusion, we have grown single crystalline Co₂FeAl films with B2 structure by MBE. The films exhibit a combination of uniaxial and cubic anisotropy. As the first direct observation of spin polarization for the Co₂FeAl system, a high spin polarization of 58% ($\pm 7\%$) at the Fermi edge at room temperature was obtained by *in-situ* spin-resolved ARPES for a 21 uc-thick Co₂FeAl film. *In-situ* MOKE measurements indicate that the thickness of the Co₂FeAl film must reach at least 4 uc to achieve both a bulk magnetization and a high surface spin polarization with only a weak thickness dependence. Our work paves the way for the design and application of spintronic devices based on Co₂FeAl films.

Methods

Epitaxial growth. To prepare the samples, we have used highly insulating GaAs (001) epi-ready wafers whose lattice constant is very close to Co₂FeAl (001)²⁸, and the Co₂FeAl thin films were grown in an ultra-high vacuum MBE system with the base pressure below 3×10^{-9} mbar. Before the growth, GaAs (001) substrates were annealed at 580 °C to remove Gallium oxide. We used two e-beam evaporators for Co and Fe and a Knudsen cell for Al with the substrate sitting at 250 °C. The deposition rate of ~ 1 uc per min was measured by a quartz microbalance, which was calibrated by thickness measurements using atomic force microscopy (AFM).

Structural characterization. The crystal structure was examined by a high resolution single crystal X-ray diffractometer (Bruker D8 Discover). The incident X-ray is from Cu-K α emission and has a wavelength of 1.5418 Å. The scan mode is θ - 2θ .

***In-situ* MOKE Characterization.** The MOKE loops were collected during growth in the longitudinal geometry using an electromagnet with a maximum field of 500 Oe, and an intensity stabilized HeNe laser (633 nm) at 300 K. The MOKE signal is proportional to the Kerr effect, the angle between the polarizer and the analyzer, and the intensity of the light. During the *in-situ* MOKE measurement, care was taken not to move any optical components in order to keep the laser intensity constant^{16,21}.

Spin-arpes measurements. *In-situ* Spin-ARPES measurements were performed using a lab-based Spin-ARPES system consisting of a SPECS PHOIBOS 150 hemisphere analyzer with 3D Micro-Mott detector and UVS 300 helium lamp (21.2 eV). The 3D Micro-Mott detector is equipped with 4 channels which allows us to measure both in-plane and out-of-plane spin components with an energy resolution of 150 meV at room

temperature. We operated the Mott detector at a scattering energy of 25 keV, and an inelastic energy window equal to 800 eV, which leads to a Sherman function of 0.16 ± 0.01 . The spectrometer was fixed at a large acceptance angle ($\pm 15^\circ$), which covered the complete Brillouin zone. The base pressure in Spin-ARPES chamber is better than 3×10^{-10} mbar, and the samples were measured at 300 K.

References

- Bainsla, L. *et al.* Spin gapless semiconducting behavior in equiatomic quaternary CoFeMnSi Heusler alloy. *Physical Review B* **91**, 104408 (2015).
- Balke, B. *et al.* Properties of the quaternary half-metal-type Heusler alloy $\text{Co}_2\text{Mn}_{1-x}\text{Fe}_x\text{Si}$. *Physical Review B* **74**, 104405 (2006).
- Cinchetti, M. *et al.* Towards a full Heusler alloy showing room temperature half-metallicity at the surface. *Journal of Physics D: Applied Physics* **40**, 1544–1547 (2007).
- Fetzer, R. *et al.* Structural, chemical, and electronic properties of the $\text{Co}_2\text{MnSi}(001)/\text{MgO}$ interface. *Physical Review B* **87**, 184418 (2013).
- Gabor, M. *et al.* Correlations between structural, electronic transport, and magnetic properties of $\text{Co}_2\text{FeAl}_{0.5}\text{Si}_{0.5}$ Heusler alloy epitaxial thin films. *Physical Review B* **92**, 054433 (2015).
- Jourdan, M. *et al.* Direct observation of half-metallicity in the Heusler compound Co_2MnSi . *Nature communications* **5**, 3974 (2014).
- Wüstenberg, J.-P. *et al.* Effects of post-growth annealing on structural and compositional properties of the $\text{Co}_2\text{Cr}_{0.6}\text{Fe}_{0.4}\text{Al}$ surface and its relevance for the surface electron spin polarization. *Journal of Physics D: Applied Physics* **42**, 084016 (2009).
- Claydon, J. S. *et al.* Element specific investigation of ultrathin $\text{Co}_2\text{MnGa}/\text{GaAs}$ heterostructures. *J Appl Phys* **101**, 09J506 (2007).
- Grabis, J., Bergmann, A., Nefedov, A., Westerholt, K. & Zabel, H. Element-specific x-ray circular magnetic dichroism of Co_2MnGe Heusler thin films. *Physical Review B* **72**, 024437 (2005).
- Scheike, T. *et al.* Chemical ordering and large tunnel magnetoresistance in $\text{Co}_2\text{FeAl}/\text{MgAl}_2\text{O}_4/\text{Co}_2\text{FeAl}$ (001) junctions. *Applied Physics Express* **9**, 053004 (2016).
- Ebke, D. *et al.* Low B2 crystallization temperature and high tunnel magnetoresistance in $\text{Co}_2\text{FeAl}/\text{MgO}/\text{Co}-\text{Fe}$ magnetic tunnel junctions. *J Magn Magn Mater* **322**, 996–998 (2010).
- Tezuka, N., Ikeda, N., Mitsuhashi, F. & Sugimoto, S. Improved tunnel magnetoresistance of magnetic tunnel junctions with Heusler $\text{Co}_2\text{FeAl}_{0.5}\text{Si}_{0.5}$ electrodes fabricated by molecular beam epitaxy. *Appl Phys Lett* **94**, 162504 (2009).
- Bowen, M. *et al.* Half-metallicity proven using fully spin-polarized tunnelling. *Journal of Physics: Condensed Matter* **17**, L407–L409 (2005).
- Andrieu, S. *et al.* Direct evidence for minority spin gap in the Co_2MnSi Heusler compound. *Physical Review B* **93**, 094417 (2016).
- Bonell, F. *et al.* Spin-polarized electron tunneling in bcc $\text{FeCo}/\text{MgO}/\text{FeCo}(001)$ magnetic tunnel junctions. *Phys Rev Lett* **108**, 176602 (2012).
- Xu, Y. B. *et al.* Evolution of the ferromagnetic phase of ultrathin Fe films grown on $\text{GaAs}(100)-4 \times 6$. *Physical Review B* **58**, 890–896 (1998).
- Gabor, M. S., Petrisor, T., Tiusan, C. & Petrisor, T. Perpendicular magnetic anisotropy in $\text{Ta}/\text{Co}_2\text{FeAl}/\text{MgO}$ multilayers. *J Appl Phys* **114**, 063905 (2013).
- Gabor, M. S., Petrisor, T., Tiusan, C., Hehn, M. & Petrisor, T. Magnetic and structural anisotropies of Co_2FeAl Heusler alloy epitaxial thin films. *Physical Review B* **84**, 134413 (2011).
- Schneider, H. *et al.* Epitaxial film growth and magnetic properties of Co_2FeSi . *Physical Review B* **74**, 174426 (2006).
- Mavropoulos, P., Lounis, S. & Blügel, S. Exchange coupling in transition-metal nanoclusters on $\text{Cu}(001)$ and $\text{Cu}(111)$ surfaces. *physica status solidi (b)* **247**, 1187–1196 (2010).
- Wang, W. H. *et al.* Magnetic properties and spin polarization of Co_2MnSi Heusler alloy thin films epitaxially grown on $\text{GaAs}(001)$. *Physical Review B* **71**, 144416 (2005).
- Anderson, G. W. Epitaxial growth of Fe on sulphur-passivated $\text{GaAs}(100)$: a method for preventing As interdiffusion. *Surf Sci* **346**, 145–157 (1996).
- Wang, X. *et al.* Structural, magnetic and transport properties of Co_2FeAl Heusler films with varying thickness. *J Magn Magn Mater* **362**, 52–57 (2014).
- Pan, Z. H. *et al.* Electronic structure of the topological insulator Bi_2Se_3 using angle-resolved photoemission spectroscopy: evidence for a nearly full surface spin polarization. *Phys Rev Lett* **106**, 257004 (2011).
- Huang, T., Cheng, X.-m., Guan, X.-w. & Miao, X.-s. Improvement of the Half-Metallic Stability of Co_2FeAl Heusler Alloys by GeTe-Doping. *IEEE T Magn* **51**, 1–4 (2015).
- Zhu, W., Sinkovic, B., Vescovo, E., Tanaka, C. & Moodera, J. S. Spin-resolved density of states at the surface of NiMnSb . *Physical Review B* **64**, 060403 (2001).
- Picozzi, S., Continenza, A. & Freeman, A. J. Role of structural defects on the half-metallic character of Co_2MnGe and Co_2MnSi Heusler alloys. *Physical Review B* **69**, 094423 (2004).
- Qiao, S., Nie, S., Zhao, J. & Zhang, X. Temperature dependent magnetic anisotropy of epitaxial Co_2FeAl films grown on GaAs . *J Appl Phys* **117**, 093904 (2015).

Acknowledgements

This work is supported by the National Key Research and Development Program of China (No. 2016YFA0300803), the National Basic Research Program of China (No. 2014CB921101), the National Natural Science Foundation of China (No. 61427812, 11774160, 11574137, 61474061, 61674079), Jiangsu Shuangchuang Program and the Natural Science Foundation of Jiangsu Province of China (No. BK20140054).

Author Contributions

L.H., Y.B.X., W.Q.L. and X.Q.Z. designed the research and co-wrote the paper. X.Q.Z. and B.L.L. fabricated the films. X.Q.Z. and X.Y.L. carried out the MOKE measurements. C.Y.G. and Y.F.N. did the XRD measurements. Y.Q.C., W.N. and X.F.W. carried out the VSM measurements. X.Q.Z., H.F.X., Q.S.L. and C.L. did the ARPES measurements. All authors commented on the final paper.

Additional Information

Supplementary information accompanies this paper at <https://doi.org/10.1038/s41598-018-26285-9>.

Competing Interests: The authors declare no competing interests.

Publisher's note: Springer Nature remains neutral with regard to jurisdictional claims in published maps and institutional affiliations.



Open Access This article is licensed under a Creative Commons Attribution 4.0 International License, which permits use, sharing, adaptation, distribution and reproduction in any medium or format, as long as you give appropriate credit to the original author(s) and the source, provide a link to the Creative Commons license, and indicate if changes were made. The images or other third party material in this article are included in the article's Creative Commons license, unless indicated otherwise in a credit line to the material. If material is not included in the article's Creative Commons license and your intended use is not permitted by statutory regulation or exceeds the permitted use, you will need to obtain permission directly from the copyright holder. To view a copy of this license, visit <http://creativecommons.org/licenses/by/4.0/>.

© The Author(s) 2018